Electronic and Infrared Spectroscopy of Anthranilic Acid in a Supersonic Jet

Cathrine A. Southern[†] and Donald H. Levy*

Department of Chemistry and the James Franck Institute, 5640 Ellis Avenue, University of Chicago, Chicago, Illinois 60637

Gina M. Florio,[§] Asier Longarte, and Timothy S. Zwier*

Department of Chemistry, 560 Oval Drive, Purdue University, West Lafayette, Indiana 47907-2084

Received: September 20, 2002; In Final Form: March 18, 2003

The electronic and infrared spectra of anthranilic acid in a supersonic jet were measured. The fluorescence excitation spectrum is extremely congested. IR−UV hole-burning measurements indicate that only a single ground-state rotamer contributes to the observed spectrum. Vibrational progressions in 252 and 418 cm^{-1} modes were observed. Density functional theory calculations indicate that these modes involve the in-plane bending motions of the amino and carboxyl groups of anthranilic acid. The presence of vibrational progressions in these modes suggests that the relative positions of the amino and carboxyl groups are different in the ground and excited electronic states of anthranilic acid. This observation is supported by the fluorescence-dip infrared spectra acquired, which show a shift in the lower frequency NH stretch fundamental from 3394 to 2900 cm^{-1} upon electronic excitation, suggesting a dramatic strengthening of the intramolecular hydrogen bond in the excited state. The change in the hydrogen-bond strength does not lead to full excited-state intramolecular hydrogen-atom transfer, as the strongly red-shifted emission feature associated with this process is not observed. Instead, the excited-state behavior of anthranilic acid is best described as intramolecular hydrogen-atom dislocation, as has been postulated for the related molecule salicylic acid.

I. Introduction

Anthranilic acid (*o*-aminobenzoic acid) is a fluorescent label used in fluorescence resonance energy transfer (FRET) studies and enzymatic cleavage assays. Solution studies show that the fluorescence behavior of anthranilic acid is different in polar and nonpolar environments.[1] Its fluorescent properties also depend on the amino acid to which it is bound.[2] In general, these variations are slight. However, when bound to proline and tryptophan the fluorescence quantum yield of anthranilic acid decreases by an order of magnitude.[2] The reasons for the observed behavior of anthranilic acid in solution are not well understood. To gain a better understanding of the intrinsic photophysical behavior of anthranilic acid, we have studied the electronic spectroscopy of this molecule in the isolated environment of a supersonic expansion.

In addition to observing the electronic spectroscopy of this molecule, we have examined the infrared spectra of anthranilic acid in both its ground and excited electronic states to study its hydrogen-bonding properties. Anthranilic acid has an intramolecular hydrogen bond between its amino and carboxyl groups. This structure is similar to that of salicylic acid, which is also known to possess an intramolecular hydrogen bond and is thought to undergo excited-state intramolecular hydrogen-atom transfer. Both anthranilic acid and salicylic acid are shown in Figure 1. The conclusion that hydrogen-atom transfer occurs in salicylic acid is based on the early work of Albert Weller. Weller postulated that proton transfer occurs in methyl salicylate (the methyl ester of salicylic acid) to explain the dual fluorescence observed in the emission spectrum of this molecule.[3,4] Methyl salicylate can transfer its hydrogen atom from the phenolic oxygen to the carbonyl oxygen, as depicted in Figure 2. Weller suggested that the weakly Stokes-shifted band observed was due to the normal (enol) tautomer whereas the strongly Stokes-shifted band resulted from the proton-transferred (keto) species and explained the process in terms of asymmetric double-well potentials in both the ground and excited electronic states. The observation of a strongly Stokes-shifted emission

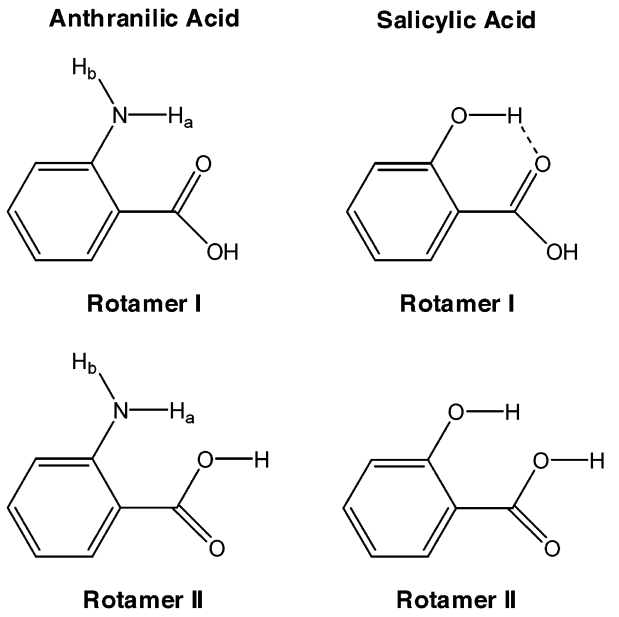

Figure 1. Structures of rotamers I and II of anthranilic acid and salicylic acid. The two amino hydrogens of anthranilic acid are labeled H_a and H_b, with H_a being the hydrogen atom closest to the carboxyl group.

* Corresponding authors. E-mail: levy@silly.uchicago.edu. Phone: 773-702-7196. E-mail: zwier@purdue.edu. Phone: 765-494-5278.

[†] Current address: Department of Chemistry, Amherst College, Amherst, MA 01002.

[§] Current address: Department of Chemistry, Columbia University, New York, NY 10027.

10.1021/jp027041x CCC: $25.00 © 2003 American Chemical Society
Published on Web 04/22/2003

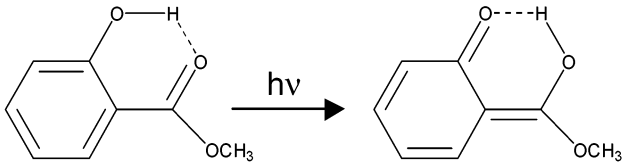

Figure 2. Enol-keto excited-state intramolecular hydrogen-atom transfer process.

feature is now the signature for an excited-state intramolecular proton (or hydrogen-atom) transfer process.

Weller believed that the excited-state product was a zwitterion, leading to his description of this process as a proton transfer. Although this terminology is still frequently applied, calculations indicate that the excited-state dynamics of salicylic acid involve the motion of a neutral hydrogen atom, rather than a proton.[5] Therefore, throughout this paper the term hydrogen-atom transfer will be used rather than proton transfer.

Recent experimental and theoretical results have called into question whether hydrogen-atom transfer actually occurs in salicylic acid. Calculations by Sobolewski and Domcke demonstrate that the excited-state potential energy surface has only a single minimum, which lies between the structures expected for the keto and enol forms of salicylic acid.[5,6] The geometry change that gives rise to the strongly Stokes-shifted emission is the result of the rearrangement of the atoms in the hydrogen-bonded ring, which is termed a hydrogen-atom dislocation, rather than a full hydrogen-atom transfer process.[5−7] This hydrogen-atom dislocation involves a lengthening of the phenolic OH bond by 0.15 Å.[5] The interpretation of Bisht et al. regarding the supersonic jet spectroscopy of salicylic acid also suggests that only a partial transfer of the hydrogen atom occurs.[8] However, following the speculation of Nagaoka et al.,[7,9] Bisht et al. state that the change in the geometry between the ground and excited electronic states is primarily localized on the benzene ring. Sobolewski and Domcke emphasize that their calculations predict that the geometry change primarily involves the heavy atoms of the hydrogen-bonded ring, not the atoms of the benzene ring.[5]

The results of recent fluorescence-dip infrared (FDIR) experiments on salicylic acid in both its ground and excited electronic states[10] are consistent with the increase in the phenolic OH bond length predicted by the calculations of Sobolewski and Domcke. The phenolic OH stretch of salicylic acid was not observed in the excited-state FDIR spectrum in the range 2400−3600 cm^{-1}. Calculations indicated that a change in OH bond length of 0.15 Å would shift the OH stretching frequency to below 2400 cm^{-1}, which was the limit of the IR laser system used. However, because the OH stretch was not actually observed, the authors concluded that their experiment does not discount the traditional view that excited-state intramolecular hydrogen-atom transfer occurs in salicylic acid.[10] It is possible that the excited-state stretch would be observable for a molecule with a weaker intramolecular hydrogen bond. As amino groups are weaker proton donors than hydroxyl groups, the intramolecular hydrogen bond present in anthranilic acid is expected to be weaker than that present in salicylic acid. It is, therefore, plausible that the hydrogen-bonded NH stretch could be observed in the excited state of anthranilic acid, providing a clearer picture of the impact of electronic excitation on an intramolecular hydrogen bond.

Experimental studies of anthranilic acid and its derivatives[11−15] are less prevalent than those of salicylic acid and its derivatives.[3,4,7,8,10,16−26] Prior studies of molecules other than anthranilic acid that have intramolecular HNH···O═C hydrogen bonds have been performed in solution and Shpol'skii matrixes.[9,11,14,15,27−33] With only one exception, 3-amino-2-naphthoic acid,[14] the emission spectra of these molecules do not display the strongly Stokes-shifted emission associated with hydrogen-atom transfer. This is most likely due to the weakly acidic nature of the amino group, as a large Stokes shift has been observed in molecules where the acidity of the amino hydrogen was enhanced by acylation of the amino group.[15,31−33] The weakly Stokes-shifted emission observed in molecules containing intramolecular HNH···O═C hydrogen bonds does not provide a great deal of information regarding the effect of electronic excitation on the intramolecular hydrogen bond. This information can be obtained more effectively with the use of infrared spectroscopy, as this technique is sensitive to small changes in hydrogen-bond geometries.

In this paper we will present the electronic spectroscopy of anthranilic acid, including fluorescence excitation and dispersed emission spectra. As this is the first examination of anthranilic acid in a supersonic jet, we will attempt to assign the observed vibronic features with the aid of density functional theory calculations. We will also present fluorescence-dip infrared spectra of this molecule in both its ground and first-excited electronic states. The comparison of the electronic and infrared spectra of anthranilic acid with those of salicylic acid allows for the comparison of the effect of electronic excitation on NH_2 and OH groups, as well as their hydrogen bonds. The spectroscopic similarities and differences between these two molecules will be discussed.

II. Experimental Section

A. Laser-Induced Fluorescence. The apparatus used to obtain the fluorescence excitation and dispersed emission spectra has been described previously[34] and will only be described briefly here. The sample was heated to 130 °C to attain a sufficient vapor pressure; the nozzle temperature was kept about 15 °C higher than the sample temperature. The molecules were seeded into helium gas at a stagnation pressure of 3−4 bar, and the mixture was expanded into a vacuum chamber through a 50 μm orifice. The supersonic expansion was crossed with the frequency-doubled output of an Nd:YAG pumped dye laser approximately 5 mm downstream of the nozzle. Fluorescence excitation spectra were acquired by monitoring the total fluorescence signal as a function of excitation wavelength with a photomultiplier tube. Dispersed emission spectra were recorded by exciting a particular transition and detecting the fluorescence with a photomultiplier tube after dispersing it through a monochromator with a reciprocal dispersion of 4 Å/mm.

B. Two-Color Resonance-Enhanced Two-Photon Ionization (Two-Color R2PI). To obtain the R2PI spectra, the fluorescence collection optics used in the laser-induced fluorescence experiments were replaced with a reflectron time-of-flight mass spectrometer, which has been described previously.[35] The ionization potential of anthranilic acid is too large for one-color resonant two-photon ionization. Ionization was achieved by introducing the fourth harmonic of another Nd:YAG laser (266 nm) in a counter-propagating geometry. The relative timing between the two lasers was controlled with either a home-built electronic circuit or a Stanford Research Systems DG535 digital delay generator. Optimum signal was obtained for zero time delay between the two lasers. The two-color R2PI spectra were obtained by gating the detector on a particular mass and scanning the UV laser to observe the wavelengths at which enhanced signal was observed.

C. Fluorescence-Dip Infrared Spectroscopy.[36−38] Conformation-specific infrared spectra in the ground and excited electronic states were obtained using fluorescence-dip infrared (FDIR) spectroscopy. A seeded Nd:YAG-pumped optical parametric converter (LaserVision, KTA based, 10 Hz), was used to produce tunable IR radiation from 2200 to 4000 cm^{-1}. Infrared laser powers of 1−3 mJ/pulse were typical. The UV and IR laser beams were spatially overlapped approximately 5 mm from the pulsed valve, and temporally separated by approximately 100 ns, with the IR preceding the UV. To generate the ground-state FDIR spectrum, the UV laser was fixed to a particular vibronic transition in the fluorescence excitation spectrum and the total fluorescence signal was monitored. Whenever the parametric converter was resonant with an infrared transition in the hydride-stretching region, population was removed from the ground vibrational state, which resulted in a depletion in the total fluorescence signal from that level when the UV laser interrogated it. Depletions were recorded by comparing the total fluorescence signal with and without the IR laser present using active baseline subtraction.

In the excited-state FDIR experiment, the UV laser precedes the IR laser by 10−15 ns. The UV laser was tuned to a known transition in the fluorescence excitation spectrum. The IR laser then promoted the molecule to higher-lying vibrational levels within the excited electronic state. The rate of radiationless processes in the molecule is more rapid at these levels, causing a decrease in the fluorescence quantum yield relative to that of the initially excited level. By detecting the fluorescence signal with a gate positioned late in the fluorescence decay, the infrared absorptions are detected as depletions in the fluorescence signal when the IR laser is resonant with a vibrational transition in the excited electronic state. In a fashion similar to the ground-state FDIR technique, the subtraction of the total fluorescence signals with and without the IR laser present generated the excited-state FDIR spectrum.

D. IR−UV Hole-Burning Spectroscopy. IR−UV hole burning spectroscopy was used to determine whether more than one conformation of anthranilic acid was present in the expansion. It differs from FDIR spectroscopy simply by which laser source is tuned: in the IR−UV hole-burning scan the IR laser is fixed and the UV is tuned. The difference in the total fluorescence signal with and without the IR laser present is recorded as in FDIR spectroscopy. All peaks in the fluorescence excitation spectrum that originate from the same ground state that is perturbed by the hole-burn laser appear as depletions in the total fluorescence signal. In this work, both the FDIR and hole-burning spectra are plotted as negative-going peaks because they represent depletions in the total fluorescence signal.

E. Calculations. Density functional theory (DFT) calculations using the Becke 3LYP functional with a 6-31G(d,p) basis set were carried out on the ground electronic state of anthranilic acid to provide a basis of comparison with experimental results. Fully optimized structures, harmonic frequencies, and IR intensities were calculated for multiple conformations of anthranilic acid. The excited-state geometry and harmonic frequencies of the lowest energy ground-state conformer of anthranilic acid were calculated at the CIS/6-31G(d,p) level. All calculations were carried out using the Gaussian 98 suite of programs.[39]

III. Results

A. Calculations. The two lowest energy conformations of anthranilic acid are shown in Figure 1. As these conformations differ by an 180° rotation of the carboxyl group, they are labeled rotamer I and rotamer II. Their key geometrical parameters are listed in Table 1. Rotamer I is more stable than rotamer II by 3.16 kcal/mol, including the zero-point energy corrections. Similar results have been obtained for salicylic acid, in which the same level of theory (B3LYP/6-31G(d,p)) predicts an energy difference of 3.91 kcal/mol between the two rotamers.[10] A third conformer of anthranilic acid, in which a hydrogen bond exists between the hydrogen of the hydroxyl group and the lone pair of the nitrogen atom, was determined to be 8.36 kcal/mol less stable than rotamer I.

TABLE 1: Calculated Geometrical Parameters for Anthranilic Acid Rotamers[a]

	rotamer I	rotamer II	aniline	benzoic acid
R_{C-N}	1.363 Å	1.373 Å	1.398 Å	
R_{N-Ha}	1.012 Å	1.007 Å	1.001 Å	
R_{N-Hb}	1.006 Å	1.007 Å	1.001 Å	
$\theta_{Ha-N-Hb}$	120.1°	117.3°	111.5°	
D_{CCNHa}	8.5°	14.6°	25.7°	
D_{CCNHb}	−12.1°	−17.3°	−25.9°	
R_{O-H}	0.971 Å	0.972 Å		0.971 Å
$R_{C=O}$	1.229 Å	1.217 Å		1.215 Å
R_{C-O}	1.358 Å	1.372 Å		1.358 Å
$R_{N-Ha\cdots OC}$	1.924 Å	1.959 Å		
θ_{N-Ha-O}	130.5°	126.6°		

[a] Calculations were performed at the B3LYP/6-31G(d,p) level. H_a and H_b are defined in Figure 1.

Table 1 also lists geometrical parameters calculated for aniline and benzoic acid that are relevant for comparison with anthranilic acid. The geometry of the amino group of anthranilic acid is different from that observed in aniline. In general, amino-substituted benzenes have been shown to be nonplanar in the ground electronic state both experimentally[40−42] and theoretically.[43−45] The CCNH dihedral angles provide a good measure of the planarity of the amino hydrogens. In aniline these dihedral angles are approximately 26°. In the case of rotamer I of anthranilic acid, the two amino hydrogens are calculated to be closer to planar than observed in aniline, with dihedral angles of 8° and 12°. The amino hydrogen closer to the carboxyl group (H_a) is more nearly planar than the other amino hydrogen (H_b), as evidenced by the smaller dihedral angle. Additionally, in anthranilic acid the NH_a bond length is longer than the NH_b bond length by 0.006 Å. In contrast, the NH bond lengths in aniline are identical.

These differences between aniline and rotamer I of anthranilic acid indicate that the presence of the carboxyl group ortho to the amino group affects the geometry of the amino hydrogens. The carboxyl group is also affected, as seen in the longer C═O bond length observed in rotamer I relative to that of benzoic acid. The most likely cause for these effects is an intramolecular hydrogen bond between the amino hydrogen (H_a) and the carboxyl carbonyl. These effects are also observed in rotamer II, but to a lesser degree. This is not surprising, as the carbonyl group is a stronger hydrogen bond acceptor than a hydroxyl group. This difference in hydrogen-bond acceptor strength is also demonstrated by the fact that the NH···O═C distance in rotamer I is shorter than the NH···O−C distance in rotamer II.

B. Electronic Spectroscopy. The fluorescence excitation spectrum of anthranilic acid is presented in Figure 3. No additional features were observed to the red of this spectrum. There are many weak features present at low energies. These features are primarily due to anthranilic acid dimers, although some can be attributed to hot bands or clusters of anthranilic acid with the carrier gas. Those bands attributed to dimers of anthranilic acid are indicated as such in Figure 3 by asterisks.

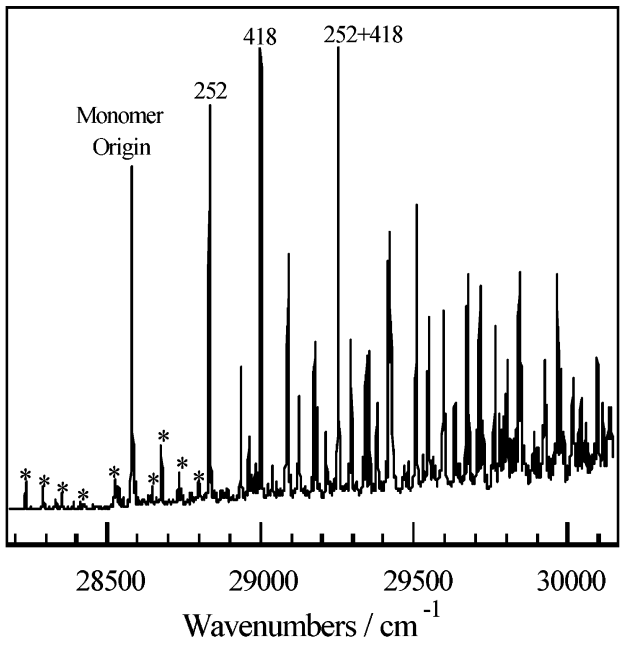

Figure 3. Fluorescence excitation spectrum of anthranilic acid in a supersonic jet. The asterisks indicate features due to anthranilic acid dimers. The monomer origin at 28 582 cm^{-1} is also indicated.

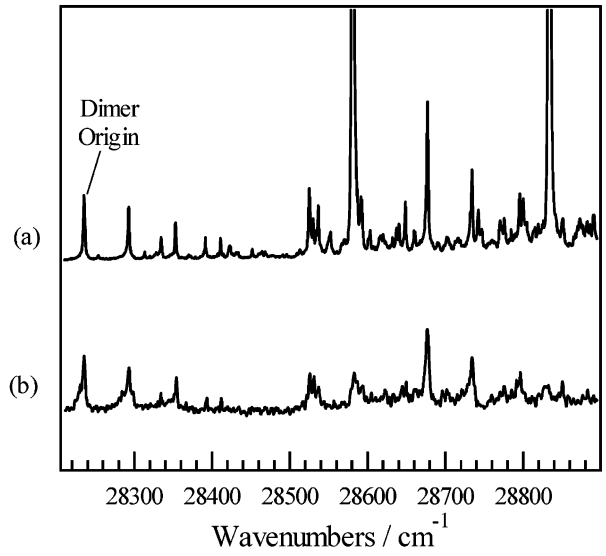

Figure 4. Comparison of (a) the fluorescence excitation spectrum of anthranilic acid with (b) the two-color, resonant two-photon ionization spectrum obtained at the dimer mass. The signals that appear in both spectra are dimer features. The dimer origin is identified as the feature at 28 233 cm^{-1}, which is 349 cm^{-1} red-shifted from the monomer origin.

The assignment of these dimer features was made by comparing the fluorescence excitation spectrum with the R2PI spectrum obtained by monitoring the signal at the dimer mass. This comparison is shown in Figure 4. With these weak features assigned, the origin of the anthranilic acid monomer can be identified as the intense feature observed at 28 582 cm^{-1}. The fluorescence excitation spectrum is highly congested, with sharp features observable only up to 2000 cm^{-1} above the origin. Starting at approximately 1500 cm^{-1} above the origin, a broad background becomes the dominant feature. The assignments of the vibrational features observed are discussed in detail in section F.

C. Fluorescence-Dip Infrared Spectroscopy Results. The fluorescence-dip infrared (FDIR) spectrum of anthranilic acid in its ground electronic state, obtained by tuning the UV laser to the electronic origin at 28 582 cm^{-1}, is shown in Figure 5a. In addition to the presence of the weak aromatic CH stretch bands typical for substituted benzene molecules, three additional features are observed. The bands at 3394 and 3542 cm^{-1} are assigned to the symmetric and antisymmetric NH_2 stretches, respectively, whereas the band at 3592 cm^{-1} is assigned to the OH stretch of the carboxyl group. The OH stretch of salicylic acid was observed at 3585 cm^{-1},[10] which is similar to the value observed in anthranilic acid, confirming this assignment.

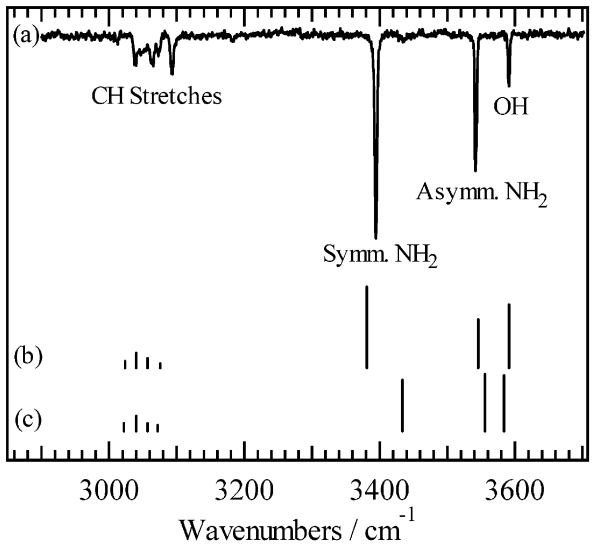

Figure 5. (a) Ground-state FDIR spectrum of anthranilic acid. (b) Calculated IR spectrum of rotamer I. (c) Calculated spectrum of rotamer II.

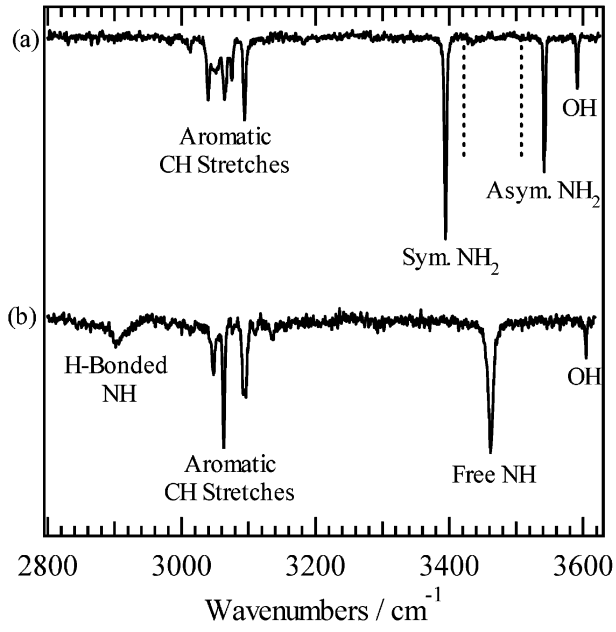

Figure 6. Comparison of the (a) ground- and (b) excited-state FDIR spectra of anthranilic acid. The dotted lines are drawn at the positions of the symmetric and antisymmetric NH_2 stretches of aniline, 3421.8 and 3508.2 cm^{-1}, respectively.[50]

The FDIR spectra of anthranilic acid in both its ground and excited electronic states are shown in Figure 6. The NH stretches observed in the excited-state spectrum differ considerably from those seen in the ground-state spectrum. One of the NH stretches occurs at a position that is approximately the average of the ground-state symmetric and antisymmetric stretches, 3460 cm^{-1}.

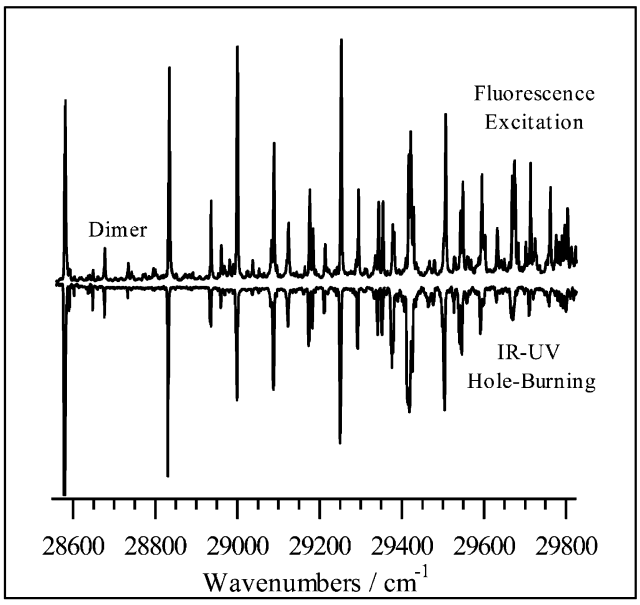

Figure 7. Comparison of the fluorescence excitation and IR−UV hole-burning spectra of anthranilic acid. As all features of the excitation spectrum are reproduced in the hole-burning spectrum, only a single conformer of anthranilic acid is observed in the region. See the text for further discussion.

The other NH stretch is assigned to the broad feature observed at approximately 2900 cm^{-1}. The carboxyl OH stretch, seen at 3604 cm^{-1}, is blue-shifted 10 cm^{-1} relative to the band position in the ground-state FDIR spectrum.

D. IR−UV Hole-Burning. One explanation for the congestion observed in the fluorescence excitation spectrum of anthranilic acid is the presence of multiple conformers in the supersonic jet. To determine the number of conformers of anthranilic acid contributing to the observed fluorescence excitation spectrum, IR−UV hole-burning experiments were performed. The IR laser was tuned to the energy of the NH_2 symmetric stretch, 3394 cm^{-1}, and the UV laser was scanned. Any feature appearing in the IR−UV hole-burning spectrum has a vibration at the frequency of the IR laser. DFT calculations predict that the NH_2 symmetric stretch frequencies of rotamers I and II differ by 53 cm^{-1}; therefore, IR−UV hole burning should be capable of distinguishing between the two rotamers. However, only one IR transition was used in the hole-burning experiments, and it is possible that there could be an accidental overlap between the NH_2 symmetric stretch frequency of rotamer I and some vibrational frequency of rotamer II.

The presence of both rotamer I and rotamer II in the jet would be indicated by the absence of spectral lines in the IR−UV hole-burning spectrum that are present in the fluorescence excitation spectrum. The comparison of the fluorescence excitation and IR−UV hole-burning spectra is shown in Figure 7. All spectral features observed in the fluorescence excitation spectrum appear in the IR−UV hole-burning spectrum, indicating that only a single conformer of anthranilic acid gives rise to the fluorescence excitation features observed in the range 28 000−29 800 cm^{-1}. The observation of only one rotamer of anthranilic acid is in contrast to salicylic acid where both rotamers were observed in a supersonic jet.[8,10] The origin transition of rotamer II of salicylic acid occurs 2280 cm^{-1} to the blue of the origin transition of rotamer I. Because only the region up to 1200 cm^{-1} above the origin of anthranilic acid was investigated, due to experimental constraints, it is possible that the rotamer II spectrum would appear at higher excitation energies. Some anthranilic acid dimer features are observed in the hole-burning spectrum because there is some overlap of the monomer and dimer NH_2 symmetric stretches. The IR−UV hole-burning spectrum acquired with the IR laser tuned to the OH stretch (data not shown) does not display these dimer features, as the OH stretches of the monomer and dimer are widely separated.

TABLE 2: Comparison of Observed and Calculated Hydride Stretch Frequencies[a]

	calcd (rotamer I)		calcd (rotamer II)		
obsd freq/cm^{-1}	freq/ cm^{-1}	int/ km mol^{-1}	freq/ cm^{-1}	int/ km mol^{-1}	assignment
3038	3024	8.9	3022	10.2	arom CH str
3063	3040	19.5	3040	19.3	arom CH str
3073	3057	12.5	3057	9.8	arom CH str
3093	3076	5.9	3072	7.8	arom CH str
3394	3381	104.1	3434	65.5	symm NH_2 str
3542	3546	62.5	3556	73.0	asymm NH_2 str
3592	3592	81.0	3584	71.3	OH str

[a] Calculations were performed at the B3LYP/6-31G(d,p) level. Frequencies have been scaled by a factor of 0.9528.

E. Comparison of Infrared Spectra and Calculations. To determine which rotamer is present in the jet, the ground-state FDIR spectrum was compared to the infrared spectra calculated for rotamers I and II. This comparison is shown in Figure 5. The calculated IR spectra have been scaled by a factor of 0.9528, a typical value for B3LYP/6-31G(d,p) calculations. Table 2 compares the experimental hydride stretch frequencies with those calculated for rotamers I and II. This comparison confirms the assignments for the hydride stretches given in section C. The IR spectrum calculated for rotamer I compares better with the experimental spectrum than the calculated result for rotamer II. The IR spectral comparison, along with the fact that rotamer I is the lowest energy conformer, allows us to assign the observed fluorescence excitation and dispersed emission spectra to rotamer I.

F. Vibrational Analysis. The above discussion indicates that the congestion in the fluorescence excitation spectrum is not due to the presence of multiple conformers but is simply the result of a large amount of Franck−Condon activity from a single conformer. There are multiple vibrational progressions present in the fluorescence excitation spectrum (Figure 3), indicating that the ground- and excited-state geometries of anthranilic acid differ along the molecular coordinates of these vibrations. In particular, the excitation spectrum is dominated by strong progressions in the 252 and 418 cm^{-1} modes, as well as combination bands of these two modes. The dispersed emission spectra obtained by exciting the anthranilic acid origin and members of the 252 cm^{-1} progression are shown in Figure 8. These spectra display progressions in the 252 and 410 cm^{-1} modes, which correspond to the 252 and 418 cm^{-1} modes present in the excitation spectrum.

To assign the vibrational features observed in both the excitation and emission spectra, the bands observed were compared to both those predicted by harmonic frequency calculations for rotamer I and those observed in related systems. This comparison and a listing of assignments are given in Table 3. The assignments of the 252 and 418 cm^{-1} modes are of greatest interest, as they provide an indication of the geometry difference between the ground and excited states. The calculations reveal that the 252 cm^{-1} mode involves the in-plane bending motion of the carboxyl group, whereas the 418 cm^{-1} mode involves the in-plane bending motions of the carbonyl and amino groups and also includes some distortion of the phenyl ring. The form of the normal modes of these vibrations

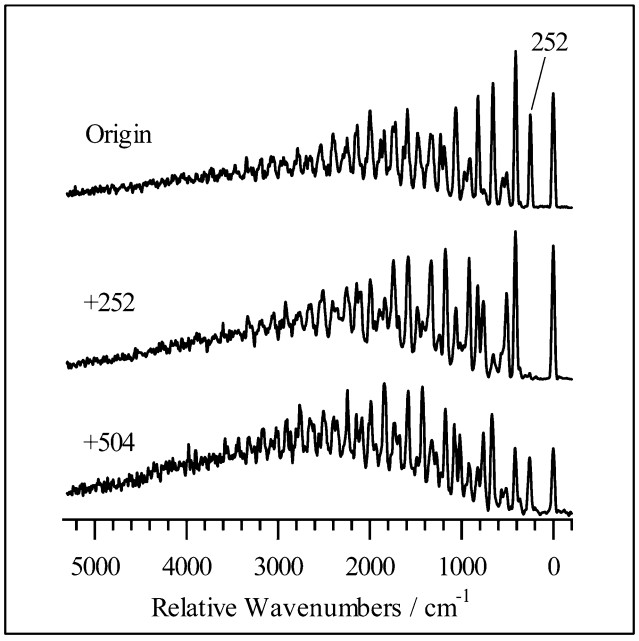

Figure 8. Dispersed emission spectra resulting from excitation of the members of the 252 cm^{-1} progression. All of these spectra are plotted relative to the excitation energy. The amount of scattered light at the excitation wavelength is negligible in all of these spectra. Spectral resolution was 0.4 nm (22−33 cm^{-1}).

TABLE 3: Frequencies of Selected Ground- and Excited-State Vibrations of Anthranilic Acid

S_0/cm^{-1}	calcd[a]/cm^{-1}	S_1/cm^{-1}	assignment
252	248	252	COOH ip bend
363	372	355	NH_2 ip bend
410	420	418	NH_2 ip bend, C=O ip bend, phenyl ring distortion
505		504	2 × 252
548	571	541	6a[b]
658		670	252 + 410 (418)
756		761	3 × 252
820		834	2 × 410 (418)
910		924	2 × 252 + 410 (418)
1017		1012	4 × 252
1230		1257	3 × 410 (418)
1635			4 × 410 (418)

[a] Calculations were performed at the B3LYP/6-31G(d,p) level. Frequencies have not been scaled. [b] Based on Wilson's notation for the vibrations of benzene. Wilson, E. B. *Phys. Rev.* **1934**, *45*, 706.

is shown in Figure 9. Emission spectra of salicylic acid display a progression in a 240 cm^{-1} mode, which Bisht et al. assigned to the in-plane bending motion of the carboxyl group,[8] in agreement with the assignment for the 252 cm^{-1} mode of anthranilic acid. Interestingly, Bisht et al. did not observe a progression in the 240 cm^{-1} mode in the excitation spectrum of salicylic acid. They assumed that the bending motion shifted to a higher frequency in the excited state, making its assignment difficult.[8]

The emission spectrum obtained by exciting the +252 cm^{-1} band (Figure 8) displays an extremely weak $v' = 1 \rightarrow v'' = 1$ transition. The same behavior is observed in the emission spectra of both the 418 cm^{-1} mode and the 418 + 252 cm^{-1} combination band. This occurrence is unusual, as the $v' = 1 \rightarrow v'' = 1$ transition is typically intense in the emission spectra of large aromatic molecules. In previous studies of *trans*-stilbene, this type of intensity distribution was observed and was attributed to a displacement of the ground- and excited-state potential energy surfaces, which causes the overlap of the $v' = 1$ and $v'' = 1$ wave functions to be nearly zero.[46] The observation of this behavior in anthranilic acid further demonstrates that the geometries of the ground and excited states differ along the coordinates of the 252 and 418 cm^{-1} vibrations.

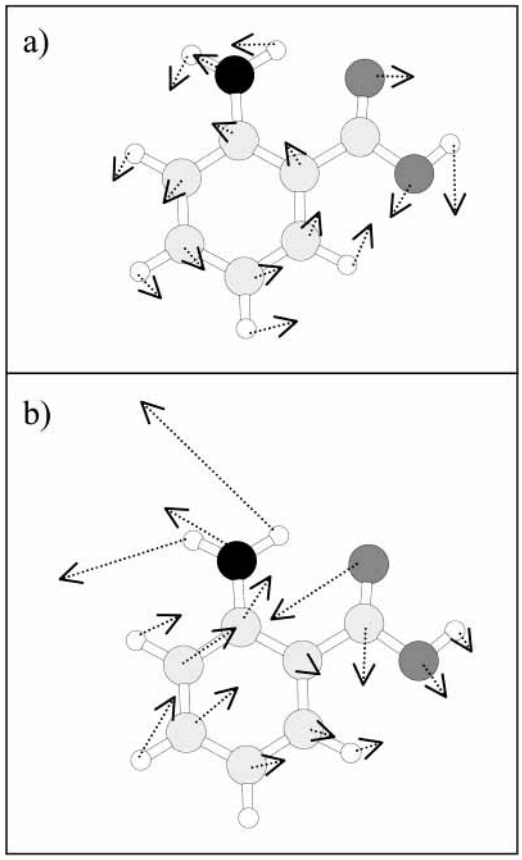

Figure 9. DFT calculated form of the normal modes assigned to the (a) 252 cm^{-1} and (b) 418 cm^{-1} vibrations. The harmonic frequencies of these modes are 248 and 420 cm^{-1}, respectively.

Franck−Condon analysis was carried out on the emission spectra of the members of the 252 cm^{-1} progression. Harmonic Franck−Condon overlap integrals can be calculated as a function of the parameters δ (the square root of the ratio of the vibrational frequencies in the ground and excited states) and D (which is proportional to the displacement of the normal coordinate upon electronic excitation[47,48]). The frequency of the 252 cm^{-1} mode, the in-plane bending motion of the carboxyl group, is unchanged in the excited electronic state, so δ has a value of 1. The parameter D was varied to find the best fit to the experimental emission spectra. The best fit was obtained for a value of D of 1.3. This value can be used to determine the accuracy of the calculated excited-state geometry of anthranilic acid. The calculation of the excited-state geometry was done at the CIS/6-31G(d,p) level.

Reimers has developed a program entitled "Dushin" that can determine the D parameter for all of the normal modes of a molecule.[49] This determination is based on the calculated geometries of the ground and excited electronic states at any level of theory. The Dushin program was applied to anthranilic acid using the ground-state geometry determined at the B3LYP/6-31G(d,p) level and the excited-state geometry calculated using the CIS method. The D parameter predicted by the Dushin program for the calculated 248 cm^{-1} mode is 0.3. The calculated 248 cm^{-1} mode corresponds to the observed 252 cm^{-1} mode, the in-plane carboxyl bend. The large discrepancy between the calculated and observed D values indicates that the excited-state geometry of anthranilic acid determined by the CIS

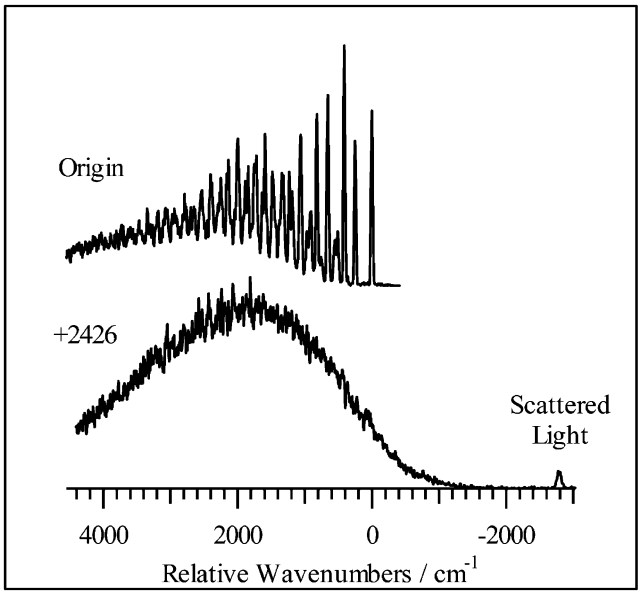

Figure 10. Comparison of the emission spectra resulting from origin excitation and excitation with 2426 cm^{-1} of excess energy. The spectra are plotted relative to the origin excitation energy. No scattered light contributes to the signal in the origin emission spectrum, whereas all of the intensity at the excitation wavelength in the +2426 cm^{-1} spectrum is due to scattered light. Spectral resolution was 0.4 nm (24−38 cm^{-1}).

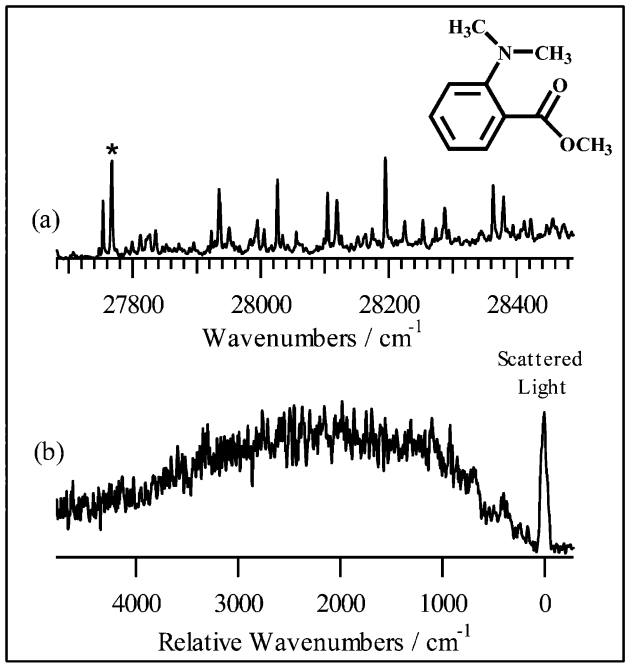

Figure 11. (a) Excitation spectrum of methyl-2-(dimethylamino)benzoate. (b) The dispersed emission spectrum that results from exciting the band indicated with an asterisk in the excitation spectrum. All of the signal at the excitation wavelength is due to scattered light. Spectral resolution was 0.4 nm (23−31 cm^{-1}).

calculation severely underestimates the geometry change along the coordinate of the in-plane carboxyl bend. Higher levels of theory must be used to more accurately determine the excited-state geometry of anthranilic acid.

With increasing excitation energy, the vibrational progressions observed in the emission spectra of anthranilic acid shown in Figure 8 are no longer visible. The dominant feature in the emission spectra resulting from excitation with 700 cm^{-1} or more of excess energy is a broad background centered approximately 2400 cm^{-1} to the red of the origin transition at 28 582 cm^{-1}. Figure 10 shows a comparison of the emission spectrum resulting from excitation with 2426 cm^{-1} of excess energy with the origin emission spectrum. The +2426 cm^{-1} emission spectrum displays only a broad band, with no sharp features present. Intermediate values of excitation energy lead to emission spectra that still retain sharp features, although they are weaker than those observed in the origin emission spectrum.

The presence of a broad, red-shifted feature is often interpreted as an indication of excited-state intramolecular hydrogen-atom transfer. To ascertain whether the broad feature observed in the emission spectra of anthranilic acid may be attributed to hydrogen-atom transfer, the emission spectrum of an anthranilic acid derivative in which hydrogen-atom transfer is not possible, methyl-2-(dimethylamino)benzoate, was examined. Hydrogen-atom transfer is prohibited in this molecule because the transferable hydrogen atoms have been replaced with methyl groups. The excitation spectrum and a representative emission spectrum of methyl-2-(dimethylamino)benzoate are shown in Figure 11. This emission spectrum shows a broad, red-shifted feature similar to that observed in the emission spectra of anthranilic acid. This indicates that the broad feature in the emission spectra of anthranilic acid is not due to hydrogen-atom transfer but is most likely the result of a combination of spectral congestion, due to the displacement of the excited-state potential relative to that of the ground state, and intramolecular vibrational energy redistribution.

IV. Discussion

The vibrational progressions observed in the fluorescence excitation and dispersed emission spectra of anthranilic acid indicate that the ground- and excited-state geometries of anthranilic acid differ along the molecular coordinates of these vibrations. The 252 and 418 cm^{-1} modes that give rise to these progressions involve the in-plane bending motions of both of the substituent groups and distortion of the phenyl ring (Figure 9). This indicates that the relative positions of the amino and carboxyl groups are altered in the electronically excited (S_1) state. One possible explanation for this geometry change is an increase in the strength of the intramolecular NH···O═C hydrogen bond in the S_1 state.

Further credence is lent to this possibility by examining the FDIR spectra of anthranilic acid. The symmetric and antisymmetric stretches of anthranilic acid in its ground electronic state occur at 3394 and 3542 cm^{-1}, respectively, as shown in Figure 6a. These frequencies are similar to those observed in aniline.[50] The dotted lines in Figure 6a show the positions of the NH_2 symmetric and antisymmetric stretches of aniline, which occur at 3421.8 and 3508.2 cm^{-1}, respectively.[50] The ground-state FDIR spectrum of rotamer I of salicylic acid displays a broad feature that occurs at a considerably lower energy, 3248 cm^{-1}, than the free OH stretch of the carboxyl group, which appears at 3585 cm^{-1}.[10] This behavior is typical for systems possessing a strong intramolecular hydrogen bond. The fact that neither of the NH_2 stretches of anthranilic acid in its ground state are broadened or strongly red-shifted relative to those of aniline indicates that the intramolecular hydrogen bond of anthranilic acid in its ground state is weak. Although the intramolecular hydrogen bond is weak, it is not nonexistent. This is demonstrated by the difference in the calculated geometries of the amino groups of aniline and anthranilic acid, which indicates an interaction between the carbonyl and amino groups. Primary amines are known to be considerably weaker hydrogen-bond

donors than hydroxyl groups, so the observation of a stronger hydrogen bond in salicylic acid than in anthranilic acid is not surprising.

Although the ground-state infrared spectra of anthranilic acid and salicylic acid suggest very different hydrogen-bonding properties, the excited-state FDIR spectra of the two molecules show similar behavior. The excited-state FDIR spectrum of anthranilic acid (Figure 6b) shows both an NH stretch with a frequency that is approximately the average of the two ground-state NH_2 stretching frequencies, and another NH stretch at a much lower energy. This can be explained by a strengthening of the intramolecular hydrogen bond of anthranilic acid in the excited state, which would cause the two NH groups to decouple, producing one stretch with a frequency that is the average of the ground-state NH_2 symmetric and antisymmetric stretches and another shifted to considerably lower frequency. The broad band at 2900 cm^{-1} is attributed to the NH stretch of the hydrogen involved in a strong intramolecular hydrogen bond. The frequency shift of this band relative to that observed in the ground-state spectrum is nearly 500 cm^{-1}, which indicates a considerable change in the properties of this hydrogen bond upon electronic excitation.

The excited-state FDIR spectrum of salicylic acid also indicates a dramatic change in the properties of the intramolecular hydrogen bond between the phenolic OH group and the carboxyl carbonyl. The S_1 FDIR spectrum of this molecule shows only the free OH stretch of the carboxyl group; the stretch of the phenolic OH was not observed in the range accessible by the IR laser, 2400−3600 cm^{-1}.[10] This was explained by a calculation of the change in OH stretching frequency with increasing OH bond length, which indicated that a change of 0.15 Å, the amount predicted by the calculations of Sobolewski and Domcke,[5] would reduce the vibrational frequency to less than 2400 cm^{-1}.[10] The extreme reduction in the frequency of the OH stretch, by over 800 cm^{-1}, is similar to the large frequency change observed for the hydrogen-bonded NH stretch of anthranilic acid.

A major spectroscopic difference between anthranilic acid and salicylic acid lies in their emission spectra. The emission spectra of anthranilic acid lack a strongly Stokes-shifted feature, which is in contrast to the dual emission observed in salicylic acid.[8,17,20−22,24] Though the strongly Stokes-shifted fluorescence observed in salicylic acid has traditionally been attributed to excited-state intramolecular hydrogen-atom transfer, the calculations of Sobolewski and Domcke indicate that a rearrangement of the atoms in the hydrogen-bonded ring may actually be responsible for this emission band.[5] In particular, their calculations predict that the difference in the geometry of the ground and excited states of salicylic acid is primarily along the molecular coordinates of the OH stretch and the in-plane bend of the carboxyl group.[5] The emission spectra of anthranilic acid display a strong progression in the in-plane bending motion of the carboxyl group, indicating a change in geometry along this coordinate, but not a large Stokes shift. This demonstrates that the primary difference in the excited-state behavior of anthranilic acid and salicylic acid is the extent of the geometry change of the atoms in the hydrogen-bonded ring.

In the case of salicylic acid, the excited-state behavior of the intramolecular hydrogen bond has been termed hydrogen-atom dislocation rather than hydrogen-atom transfer.[5−7] This process involves the rearrangement of the hydrogen-bonded ring, including a strengthening of the intramolecular hydrogen bond, but falls short of the full transfer of the hydrogen atom. A similar terminology can be applied to the case of anthranilic acid, as indicated by both the red shift of the hydrogen-bonded NH stretching frequency and the fact that progressions in modes involving the atoms present in the hydrogen-bonded ring dominate the excitation and emission spectra.

A final difference observed between salicylic acid and anthranilic acid is the fact that two conformers of salicylic acid have been observed,[8,10] whereas only one of anthranilic acid has been identified thus far. UV−UV hole-burning studies are more conclusive than IR−UV hole-burning in determining the number of conformers present. These experiments are currently underway to establish for certain that no other conformers of anthranilic acid are present in the supersonic jet. FDIR studies of the anthranilic acid dimer have also been performed and will be presented in a separate publication.

V. Conclusions

The combined information provided by fluorescence excitation, dispersed emission, and both ground- and excited-state FDIR spectra indicate that anthranilic acid undergoes a geometry change between its ground and first-excited electronic states, which involves the strengthening of the NH···O═C intramolecular hydrogen bond present in this molecule. A comparison of the hydrogen-bonding properties of anthranilic acid and salicylic acid shows both similarities and differences between the two molecules. Although both molecules possess an intramolecular hydrogen bond in their ground states, the hydrogen bond in salicylic acid is considerably stronger than the hydrogen bond in anthranilic acid.

Although the ground-state hydrogen-bonding properties of these molecules differ, similar effects are observed in their electronically excited states. Both molecules exhibit a dramatic change in the strength of their intramolecular hydrogen bonds upon electronic excitation, which leads to a severe reduction in the hydrogen-bonded stretching frequencies. In the case of salicylic acid, the observation of dual fluorescence has been attributed to excited-state intramolecular hydrogen-atom transfer.[3,4,8,16,21,22,24,25] Although a broad, red-shifted feature is observed in the emission spectra of anthranilic acid, the similarity of this feature to that observed in methyl-2-(dimethylamino) benzoate, and the fact that the red shift observed is only 2400 cm^{-1}, indicates that hydrogen-atom transfer does not occur in anthranilic acid. Recent calculations suggest that the primary geometry change of the excited state of salicylic acid involves the rearrangement of the hydrogen-bonded ring.[5] This type of geometry change is similar to what is suggested for anthranilic acid by the progressions observed in the excitation and emission spectra and the excited-state FDIR results. The overall findings of this work indicate that although NH···O═C hydrogen bonds are weaker than OH···O═C hydrogen bonds, both systems exhibit similar behavior upon electronic excitation.

Acknowledgment. T.S.Z., G.M.F., and A.L. gratefully acknowledge the NSF for support of this work under grant CHE9728636. We also acknowledge the assistance of Jasper Clarkson. C.A.S and D.H.L. acknowledge Dave Gordon for suggesting the study of anthranilic acid. We are grateful to J. R. Reimers for providing a copy of the computer program Dushin that was used in this work.

References and Notes

(1) Turchiello, R. F.; Lamy-Freund, M. T.; Hirata, I. Y.; Juliano, L.; Ito, A. S. *Biophys. Chem.* **1998**, *73*, 217−225.

(2) Ito, A. S.; Turchiello, R. D. F.; Hirata, I. Y.; Cezari, M. H. S.; Meldal, M.; Juliano, L. *Biospectroscopy* **1998**, *4*, 395−402.

(3) Weller, A. *Prog. React. Kinet. Mech.* **1961**, *1*, 187−214.

(4) Weller, A. *Z. Elektrochem.* **1956**, *60*, 1144−1147.
(5) Sobolewski, A. L.; Domcke, W. *Chem. Phys.* **1998**, *232*, 257−265.
(6) Sobolewski, A. L.; Domcke, W. *Phys. Chem. Chem. Phys.* **1999**, *1*, 3065−3072.
(7) Nagaoka, S.; Nagashima, U. *Chem. Phys.* **1989**, *136*, 153−163.
(8) Bisht, P. B.; Petek, H.; Yoshihara, K.; Nagashima, U. *J. Chem. Phys.* **1995**, *103*, 5290−5307.
(9) Nagaoka, S.; Nagashima, U. *Chem. Phys.* **1996**, *206*, 353−362.
(10) Yahagi, T.; Fujii, A.; Ebata, T.; Mikami, N. *J. Phys. Chem. A* **2001**, *105*, 10673−10680.
(11) Hambly, A. N.; O'Grady, B. V. *Aust. J. Chem.* **1963**, *16*, 459−474.
(12) Tramer, A. *J. Mol. Struct.* **1969**, *4*, 313−325.
(13) Tramer, A. *J. Phys. Chem.* **1970**, *74*, 887−894.
(14) Srivastava, S.; Dogra, S. K. *J. Photochem. Photobiol. A-Chem.* **1989**, *46*, 329−345.
(15) Yoshihara, T.; Shimada, H.; Shizuka, H.; Tobita, S. *Phys. Chem. Chem. Phys.* **2001**, *3*, 4972−4978.
(16) Bisht, P. B.; Okamoto, M.; Hirayama, S. *J. Phys. Chem. B* **1997**, *101*, 8850−8855.
(17) Denisov, G. S.; Golubev, N. S.; Schreiber, V. M.; Shajakhmedov, S. S.; Shurukhina, A. V. *J. Mol. Struct.* **1997**, *437*, 153−160.
(18) Heimbrook, L.; Kenny, J. E.; Kohler, B. E.; Scott, G. W. *J. Phys. Chem.* **1983**, *87*, 280−289.
(19) Heimbrook, L. A.; Kenny, J. E.; Kohler, B. E.; Scott, G. W. *J. Chem. Phys.* **1981**, *75*, 5201−5203.
(20) Joshi, H. C.; Mishra, H.; Tripathi, H. B. *J. Photochem. Photobiol. A-Chem.* **1997**, *105*, 15−20.
(21) Lahmani, F.; Zehnacker-Rentien, A. *Chem. Phys. Lett.* **1997**, *271*, 6−14.
(22) Lahmani, F.; Zehnacker-Rentien, A. *J. Phys. Chem. A* **1997**, *101*, 6141−6147.
(23) Lopez-Delgado, R.; Lazare, S. *J. Phys. Chem.* **1981**, *85*, 763−768.
(24) Pant, D. D.; Joshi, H. C.; Bisht, P. B.; Tripathi, H. B. *Chem. Phys.* **1994**, *185*, 137−144.
(25) Catalan, J.; Tomas, F. *Adv. Mol. Relax. Processes* **1976**, *8*, 87−94.
(26) Kuper, J. W.; Perry, D. S. *J. Chem. Phys.* **1984**, *80*, 4640−4645.
(27) Balakrishnan, N.; Gillispie, G. D. *J. Phys. Chem.* **1989**, *93*, 2337−2341.
(28) Carter, T. P.; Vanbenthem, M. H.; Gillispie, G. D. *J. Phys. Chem.* **1983**, *87*, 1891−1898.
(29) Flom, S. R.; Barbara, P. F. *J. Phys. Chem.* **1985**, *89*, 4489−4494.
(30) Gillispie, G. D.; Balakrishnan, N.; Johnson, D. E. *J. Phys. Chem.* **1989**, *93*, 2334−2336.
(31) Neuwahl, F. V. R.; Bussotti, L.; Righini, R.; Buntinx, G. *Phys. Chem. Chem. Phys.* **2001**, *3*, 1277−1283.
(32) Smith, T. P.; Zaklika, K. A.; Thakur, K.; Barbara, P. F. *J. Am. Chem. Soc.* **1991**, *113*, 4035−4036.
(33) Smith, T. P.; Zaklika, K. A.; Thakur, K.; Walker, G. C.; Tominaga, K.; Barbara, P. F. *J. Phys. Chem.* **1991**, *95*, 10465−10475.
(34) Smalley, R. E.; Levy, D. H.; Wharton, L. *J. Chem. Phys.* **1976**, *64*, 3266−3276.
(35) Carrasquillo, E.; Zwier, T. S.; Levy, D. H. *J. Chem. Phys.* **1985**, *83*, 4990−4999.
(36) Ebata, T.; Fujii, A.; Mikami, N. *Int. Rev. Phys. Chem.* **1998**, *17*, 331−361.
(37) Frost, R. K.; Hagemeister, F. C.; Arrington, C. A.; Zwier, T. S.; Jordan, K. D. *J. Chem. Phys.* **1996**, *105*, 2595−2604.
(38) Walther, T.; Bitto, H.; Minton, T. K.; Huber, J. R. *Chem. Phys. Lett.* **1994**, *231*, 64−69.
(39) Frisch, M. J.; Trucks, G. W.; Schlegel, H. B.; Scuseria, G. E.; Robb, M. A.; Cheeseman, J. R.; Zakrzewski, V. G.; Montgomery, J. A., Jr.; Stratmann, R. E.; Burant, J. C.; Dapprich, S.; Millam, J. M.; Daniels, A. D.; Kudin, K. N.; Strain, M. C.; Farkas, O.; Tomasi, J.; Barone, V.; Cossi, M.; Cammi, R.; Mennucci, B.; Pomelli, C.; Adamo, C.; Clifford, S.; Ochterski, J.; Petersson, G. A.; Ayala, P. Y.; Cui, Q.; Morokuma, K.; Malick, D. K.; Rabuck, A. D.; Raghavachari, K.; Foresman, J. B.; Cioslowski, J.; Ortiz, J. V.; Baboul, A. G.; Stefanov, B. B.; Liu, G.; Liashenko, A.; Piskorz, P.; Komaromi, I.; Gomperts, R.; Martin, R. L.; Fox, D. J.; Keith, T.; Al-Laham, M. A.; Peng, C. Y.; Nanayakkara, A.; Challacombe, M.; Gill, P. M. W.; Johnson, B.; Chen, W.; Wong, M. W.; Andres, J. L.; Gonzalez, C.; Head-Gordon, M.; Replogle, E. S.; Pople, J. A. *Gaussian 98*, revision A.9; Gaussian, Inc.: Pittsburgh, PA, 1998.
(40) Brand, J. C. D.; Williams, D. R.; Cook, T. J. *J. Mol. Spectrosc.* **1966**, *20*, 359−380.
(41) Lister, D. G.; Tyler, J. K.; Hog, J. H.; Larsen, N. W. *J. Mol. Struct.* **1974**, *23*, 253−264.
(42) Sinclair, W. E.; Pratt, D. W. *J. Chem. Phys.* **1996**, *105*, 7942−7956.
(43) Bludsky, O.; Sponer, J.; Leszczynski, J.; Spirko, V.; Hobza, P. *J. Chem. Phys.* **1996**, *105*, 11042−11050.
(44) Jiang, J. C.; Lin, C. E. *J. Mol. Struct. (THEOCHEM)* **1997**, *392*, 181−191.
(45) Lopez-Tocon, I.; Della Valle, R. G.; Becucci, M.; Castellucci, E.; Otero, J. C. *Chem. Phys. Lett.* **2000**, *327*, 45−53.
(46) Syage, J. A.; Felker, P. M.; Zewail, A. H. *J. Chem. Phys.* **1984**, *81*, 4685−4705.
(47) Coon, J. B.; Dewames, R. E.; Loyd, C. M. *J. Mol. Spectrosc.* **1962**, *8*, 285−299.
(48) Henderson, J. R.; Muramoto, M.; Willett, R. A. *J. Chem. Phys.* **1964**, *41*, 580−581.
(49) Reimers, J. R. *J. Chem. Phys.* **2001**, *115*, 9103−9109.
(50) Nakanaga, T.; Ito, F.; Miyawaki, J.; Sugawara, K.; Takeo, H. *Chem. Phys. Lett.* **1996**, *261*, 414−420.